Surface measurements by white light spatial-phase-shift imaging interferometry

Yoel Arieli,[1,*] Shlomi Epshtein,[2] Igor Yakubov,[2] Yosi Weitzman,[2] Garrett Locketz,[3] and Alon Harris[4]

[1]*Jerusalem College of Technology, Havaad Haleumi 21, Jerusalem 9372115, Israel*
[2]*AdOM Technologies, Hamlacha 1, Lod 7152001, Israel*
[3]*Tel Aviv University, Sackler School of Medicine, Tel Aviv 6997801, Israel*
[4]*Glick Eye Center, Indiana University Medical Center, Indianapolis, Indiana 46202, USA*
[*]*arieli.yoel@gmail.com*

Abstract: A novel method of common-path imaging interferometry, the White Light Spatial-Phase-Shift (WLSPS) for object surface measurements, is discussed here. Compared to standard White Light Interferometry (WLI), which uses a reference mirror, the interferometry of WLSPS is obtained by creating manipulations to the light wavefront reflected from an object's surface. Using this approach, surface measurements can be obtained from any real object image, and do not need to be taken directly from the object itself. This creates the ability for a surface measurement tool to be attached to any optical system that generates a real image of an object. Further, as this method does not require a reference beam, the surface measurement system contains inherent vibration cancelation

References and links

1. O. Soloviev and G. Vdovin, "Phase extraction from three and more interferograms registered with different unknown wavefront tilts," Opt. Express **13**(10), 3743–3753 (2005).
2. S. Cain, "Design of an image projection correlating wavefront sensor for adaptive optics," Opt. Eng. **43**(7), 1670–1681 (2004).
3. A. Shevchenko, S. C. Buchter, N. V. Tabiryan, and M. Kaivola, "Self-focusing in a nematic liquid crystal for measurements of wavefront distortions," Opt. Commun. **232**(1–6), 439–442 (2004).
4. T. Fukuchi, Y. Yamaguchi, T. Nayuki, K. Nemoto, and K. Uchino, "Development of a laser wavefront sensor for measurement of discharges in air," Electr. Eng. Jpn. **146**(4), 10–17 (2004).
5. S. Wolfling, N. Ben-Yosef, and Y. Arieli, "Generalized method for wave-front analysis," Opt. Lett. **29**(5), 462–464 (2004).
6. S. Wolfling, D. Banitt, N. Ben-Yosef, and Y. Arieli, "Innovative metrology method for the 3-dimensional measurement of MEMS structures," Proc. SPIE **5343**, 255–263 (2004).
7. S. Wolfling, E. Lanzmann, M. Israeli, N. Ben-Yosef, and Y. Arieli, "Spatial phase shift interferometry—A wavefront analysis technique for three-dimensional topometry," J. Opt. Soc. Am. A **22**(11), 2498–2509 (2005).
8. D. W. Phillion, "General methods for generating phase-shifting interferometry algorithms," Appl. Opt. **36**(31), 8098–8115 (1997).
9. F. Zernike, "Diffraction theory of knife-edge test and its improved form, the phase-contrast," Mon. Not. R. Astron. Soc. **94**, 377–384 (1934).
10. R. Jensen-Clem, J. K. Wallace, and E. Serabyn, "Characterization of the phase shifting Zernike wavefront sensor for telescope applications," in *Aerospace Conference* (IEEE, 2012), pp. 1–7.
11. J. C. Wyant, "White light interferometry," Proc. SPIE **4737**, 98–107 (2002).
12. K. Underwood, J. C. Wyant, and C. L. Koliopoulos, "Self-referencing wavefront sensor," Proc. SPIE **0351**, 108–114 (1983).

1. Introduction

In recent years, new quantitative methods for wavefront phase measurement have been undertaken [1–4]. These efforts were instigated by the need for high-accuracy wavefront analysis for surface measurement applications in microelectronics and optical components, as well as for applications in laser communication and micro-electro-mechanical systems (MEMS). In [5–7], we introduced the spatial-phase-shift (SPS) method; a novel imaging

interferometry technique for surface measurements and wavefront analysis. The SPS method is related to two different techniques: the phase-shift interferometry (PSI) technique [8] and the Zernike Phase – Contrast (ZPC) method [9]. In the SPS method, elements of the PSI and ZPC methods are combined in the sense that the ZPC setup is used while various controlled phase changes are introduced as in the PSI instead of a fixed phase change. This method was published again as the Phase Shifting Zernike Interferometer [10]. Like the ZPC method, the SPS method also utilizes common-path interferometry and thus is inherently vibration insensitive. In addition, because of the imaging implementation of the method, the SPS method can be used to analyze an imaged wavefront, thus enabling it to be added as a measurement sensor to any optical system that images unaberrated wavefronts.

In this paper, we extend the SPS to combine the ZPC method with White Light Interferometry (WLI) [11], and thus introduce a broadband light source, instead of using monochromatic light. White light fringes are obtained by dividing the wavefront reflected from the object to two parts and introducing a continuous phase delay to one part of the wavefront relative to the other.

2. White light spatial-phase-shift

The basic optical system for measuring an object's surface by the White Light Spatial-Phase-Shift (WLSPS) method is the traditional 4F optical system, shown in Fig. 1. The object to be measured is placed in the front focal plane of the first lens having a focal length F and is illuminated normally by a collimated broadband light beam.
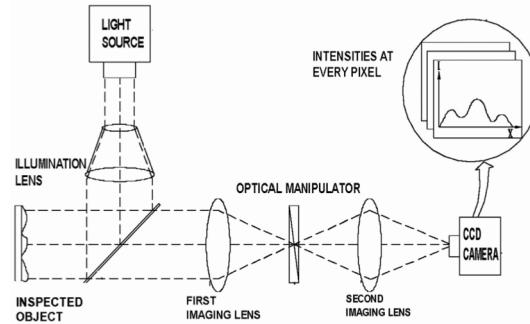
Fig. 1. General characteristic optical setup of the WLSPS interferometry technique.

For each wavelength, the complex amplitude of the wavefront reflected from the object is:

$$o(x, y, \lambda) = A(x, y, \lambda) \exp\left[i\varphi(x, y, \lambda)\right] \qquad (1)$$

where A is the reflected amplitude and φ is the phase of each wavefront.

To the first approximation, the phase map $\varphi(x, y, \lambda)$ of each wavefront is related to the height map $h(x, y, \lambda)$ of the object by:

$$\varphi(x, y, \lambda) = -4\pi \frac{h(x, y)}{\lambda} \mod 2\pi \qquad (2)$$

where mod 2π is the phase modulo 2π.

The wavefronts are reflected from the object and collected by the first lens. In the back focal plane of the lens, the complex amplitudes of each wavelength are proportional to $O(v, u, \lambda)$ the Fourier transform of the reflected wavefronts $o(v, u, \lambda)$.

At the Fourier plane, the wavefronts are modified by an optical manipulator, and two different phase delays are introduced to two spatially distinct parts of each wavefront. Due to the dispersion, the phase difference between the two spatial parts might be wavelength-

dependent and is denoted by $\theta(\lambda)$. The two different spatial parts are characterized by the spatial functions $G(u,v)$ and $1-G(u,v)$. The spatial function $G(u,v)$ is a binary function with the values one or zero. Whenever $G(u,v)$ is one, the function $1-G(u,v)$ is zero and vice versa. Thus the modification function is:

$$H(u,v,\lambda) = G(u,v)\{\exp[i\theta(\lambda)]-1\}+1 \qquad (3)$$

In the Fourier plane, after modification, the complex amplitudes of the wavefronts are:

$$O'(u,v,\lambda) = C_1(\lambda)O(u,v,\lambda)H(u,v,\lambda) \qquad (4)$$

where C_1 is a wavelength dependent constant for a given optical system.

The modified wavefronts are retransformed by the second lens and imaged onto an image plane where a CCD camera is placed. Assuming for simplicity that the two lenses have the same focal length, the complex amplitudes at the image plane are proportional to the Fourier transform of $O'(u,v,\lambda)$:

$$
\begin{aligned}
a(x,y,\lambda) &= C_2(\lambda)F^{-1}\left[O'(u,v,\lambda)\right] \\
&= C_2(\lambda)F^{-1}\left\{C_1(\lambda)\left[O(u,v,\lambda)\right]\left[G(u,v)\{\exp[i\theta(\lambda)]-1\}+1\right]\right\} \quad (5)\\
&= C(\lambda)\left\{o(x,y,\lambda)+S(x,y,\lambda)\left[\exp(i\theta)-1\right]\right\}
\end{aligned}
$$

where C_2 is also a wavelength dependent constant for a, $C(\lambda) = C_1(\lambda)C_2(\lambda)$ and $S(x,y,\lambda) = o(x,y,\lambda)*g(x,y)$. The sign * denotes convolution.

The function $S(x,y,\lambda)$ is the two-dimensional convolution of the complex amplitude of the original wavefront $o(x,y,\lambda)$ of each wavelength with the rescaled inverse Fourier transform $g(x,y)$ of the characteristic function $G(u,v)$. $S(x,y,\lambda)$ is wavelength-dependent. Actually, the second lens operates the Fourier transform and not the inverse Fourier transform, which results in reversing the signs of the physical dimensions.

In the imaging process, the different spatial parts of the modified wavefronts interfere with each other. According to Eq. (5), the field at the image plane is the interference of the complex amplitude of the object $o(x,y,\lambda)$ with the function $S(x,y,\lambda)$ multiplied by $[\exp(i\theta)-1]$. The function $S(x,y,\lambda)$ can be considered as a reference beam and it plays a similar role to that of the reference beam in standard white light interferometry.

As the spatial dimensions of the characteristic function $G(u,v)$ decrease, the function $S(x,y,\lambda)$ spreads on the image plane, and its amplitude and phase approach constant values throughout the image plane. These constants depend on the object itself and the illumination wavelength.

From Eq. (5), it follows that the image intensity of each wavelength is:

$$I(x,y,\lambda) = \left|C(\lambda)\{o(x,y,\lambda)+S(x,y,\lambda)[\exp(i\theta)-1]\}\right|^2 \qquad (6)$$

The detector integrates the light at each pixel and the signal is:

$$I(x,y,\lambda) = R(\lambda)\int\left|C(\lambda)\{o(x,y,\lambda)+S(x,y,\lambda)[\exp(i\theta)-1]\}\right|^2 d\lambda \qquad (7)$$

where $R(\lambda)$ is the spectral responsivity of the detector.

The main difference between the WLSPS and the standard WLI is that while in the standard WLI the reference beam is uniform in its spectra and phase throughout the image plane, in the WLSPS, the complex function $S(x,y,\lambda)$ which serves as the reference beam, is wavelength-dependent, and its spectrum and phase may vary over the image plane. Further, the WLPS complex function, and thus reference beam, may also vary from object to object.

The variations in the spectrum over the image plane do not disturb the measurement process, since they can be considered as using different light sources with different spectra for each image point. However, the non-constant and wavelength-dependent phase over the image plane can be considered as the effect of a strong dispersion and may be harmful. Nevertheless, this effect can be harnessed when the light source bandwidth is limited, though at the cost of losing measurement resolution. On the other hand, since there is no need for a reference mirror and the reference beams are taken from the wavefronts themselves, two important advantages over the standard WLI are gained; the measurement process is insensitive to vibrations, and surface measurements can be applied to a real image of an object without the necessity of imaging the object itself. Thus, the measurement tool can be attached to any optical system that creates a real image of an object and can be used to measure the object's surface.

3. The WLSPS setup

The optical setup for the WLSPS is shown in Fig. 2. The setup includes two parts; the illumination and the imaging apparatuses.

The illumination apparatus includes a Philips halogen reflector lamp, EKE 150W light source and a slit. The slit was located in the focal plane of the reflector. The slit plane was imaged to infinity and a collimated beam illuminated the object. The imaging apparatus was actually an imaging system with an objective lens close to the object and an imaging lens close to the detector's plane where a CCD camera was located. Since there is no SLM that can create a long and continuous OPD, a Michelson interferometer was placed behind the objective lens as shown in Fig. 2. The beam splitter in the Michelson interferometer divided the incoming beam to two beams, each propagated in a separate arm of the interferometer. At the two interferometer mirrors, different spatial parts of the beams were blocked by annular and aperture stops, as shown in Fig. 3. The annular and the aperture stops represented the spatial functions $G(u,v)$ and $1-G(u,v)$. The interferometer mirrors' planes were located at the focal plane of the objective lens to obtain a two-dimensional Fourier transform of the object. Using Michelson interferometer requires two issues to be addressed; the vibration sensitivity and the dispersion in the Michelson beam-splitting cube. Regarding vibration sensitivity, only the OPD between the two parts of the wavefront is taken into consideration. Therefore, when the interferometer used is rigid, the OPD between the two parts of the wavefront remains constant and thus the system is still insensitive to axial vibrations. Moreover, in the current experiment, the OPD between the interferometer's arms is changed continuously, thus the vibrations of one arm relative to the other arm are not harmful. The dispersion in the Michelson beam-splitting cube only spreads the envelope of the wave packet and thus only lowers measurement resolution.

After the phase shifting, the object was imaged on the CCD plane, with X5 magnification. By moving one of the mirrors continuously, a continuous phase shift between the two beams was obtained. It should be noted that although a similar method for dividing the wavefront into two parts is described by Underwood et al. [12] using a Point Diffraction Interferometry (PDI) apparatus, the current experiment is distinguished by its implementation of a broadband light source, and by the utilization of the function $S(x,y,\lambda)$ which is considered as a reference beam and is not spherical as in the PDI.
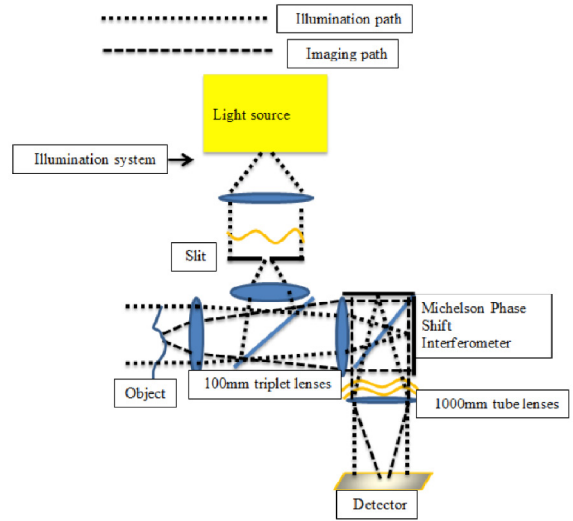
Fig. 2. The optical system for the WLSPS includes two parts, the illumination and the imaging apparatuses.
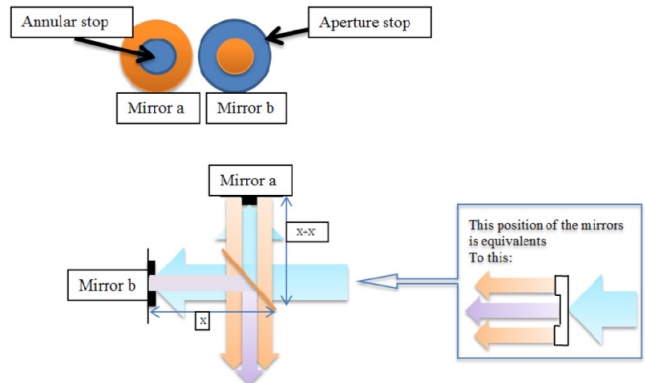
Fig. 3. The beam splitter in the Michelson interferometer divides the incoming beam to two beams, each propagated in each interferometer's arms. At the interferometer mirrors, spatial parts of the beams were blocked by an annular and an aperture stops and a phase shift is introduced.

4. Results

A VLSI target with a trench of 1 mm width and 8 μm depth was measured using the WLSPS setup described above. The VLSI target shown in Fig. 4, has a standard deviation of 26 Å over 9 measurements spaced 50 um apart on the step height bar. It can be seen that the individual parts of the VLSI target, each with distinct heights, have different illumination intensities due to the phase contrast effect.
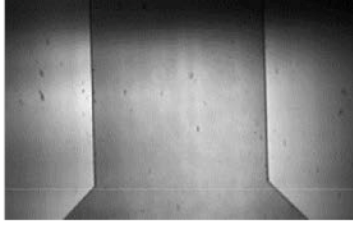
Fig. 4. The VLSI target with a trench of 1 mm width and 8 μm depth. The individual parts of the VLSI target, each with distinct heights, have different intensity illumination due to the phase contrast effect.

Continuous images of the VLSI target were taken while constantly moving one of the interferometer's mirrors. This mirror movement created a continuous phase shift between the two beams and the contrast of the images varied with time. At each point on the image, as the phase shift between the two functions $S(x,y,\lambda)$ and the complex amplitude of the object $o(x,y,\lambda)$ varied, the interferogram was created. The maximum contrast of the interferogram was obtained at a phase shift corresponding to an OPD between a point on the object's surface and a "virtual reference position" attained by the function $S(x,y,\lambda)$. A typical interferogram (raw data) is shown in Fig. 5.
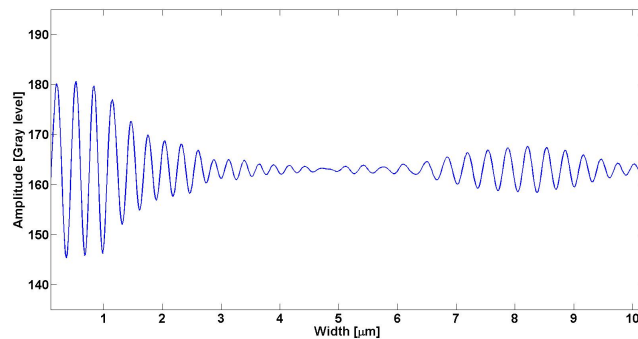
Fig. 5. A typical interferogram obtained in the WLSPS setup.

By calculating the OPDs where the maximum contrasts were obtained at each point, the three dimensional object was reconstructed. A 3D reconstruction of the VLSI is shown in Fig. 6, where all the dimensions are represented in microns. The WLSPS method yields a highly accurate reconstruction of the VLSI, where the measured depth is 8 microns with a STD of 0.115 microns.
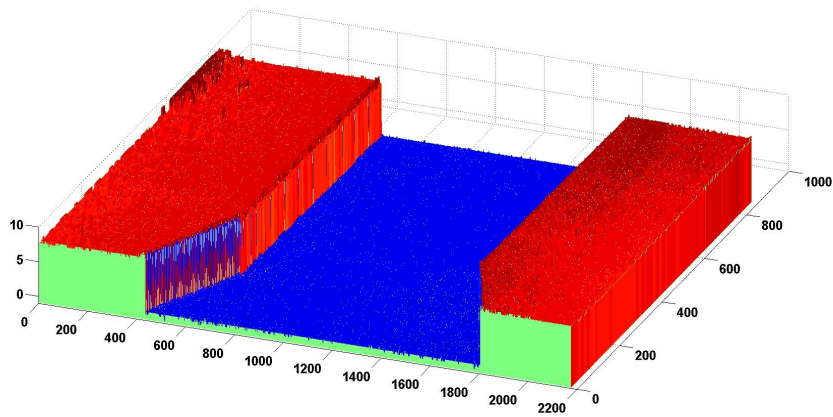
Fig. 6. A 3D reconstruction of the VLSI. All dimensions represented in microns.

5. Conclusions

An extension the SPS method is introduced via incorporation of a broadband white light source, instead of using monochromatic light. In this approach, white light fringes were obtained by dividing the wavefront reflected from an object to two parts while simultaneously introducing a continuous phase delay to one part of the wavefront relative to the other. The optical system was designed and built whereby a Michelson interferometer created a phase delay to one part of the wavefront relative to the other. A three dimensional VLSI target was measured using the setup and reconstructed. By calculating the OPDs where the maximums contrasts had obtained at each point, the three dimensional object was reconstructed. Experiments showed the VLSI was reconstructed accurately with the STD of 0.115 microns.

Acknowledgments